

# Measurement of electron density profile behind strong shock waves with a Langmuir probe

S. Wang<sup>1</sup>, J.P. Cui<sup>1</sup>, B.C. Fan<sup>1</sup>, Y.Z. He<sup>1</sup>, R.L. Zhang<sup>2</sup>, L.H. Han<sup>2</sup>,  
F.M. Yu<sup>2</sup>, and J.L. Le<sup>2</sup>

<sup>1</sup> *Laboratory of High Temperature Gas Dynamics, Institute of Mechanics,  
Chinese Academy of Sciences, Beijing 100080, China*

<sup>2</sup> *China Aerodynamic Research and Development Center,  
P.O. Box 211 Mizuyang 621000, Sichuan, China*

**Abstract.** At the shock velocity range of 7~9km/s, the variations of electron density behind strong shock waves are measured in a low-density shock tube by using the Langmuir electrostatic probe technique. The electron temperature, calculated based on Park's three-temperature model, is used in interpreting the probe current data. The peak electron densities determined in the present experiment are shown to be approximately half lower than those predicted by Lin's calculation. The experimentally obtained ratios of the characteristic ionization distance to the mean free path of freestream ahead of the shock wave are found to be in a good agreement with the existing experiments and Park's calculation.

## 1 Introduction

As we know, there are nonequilibrium dissociation, ionization and radiation in shock heating air. In order to understand and characterize the nonequilibrium ionization phenomena, many measurements of the electron density profiles behind shock waves have been made in the past decades. In air, there exist the three types of ionic reactions: 1) associative ionization of nitrogen and oxygen atoms, 2) charge-exchange reactions, and 3) the electron-impact ionization. At relatively low flight velocities (below about 6km/s), only the first mechanism is present; at the intermediate flight velocities (between 6 and 10km/s), the second mechanism is added to the first. At higher velocities (above 10km/s), the third mechanism becomes significant. However, experimental data at the intermediate shock velocity range (between 6 and 9km/s) are scarce, which corresponds to the ionization mechanism transition from the area dominated by the associative ionization of nitrogen and oxygen atoms to the area added by the charge-exchange reactions. The present work aims at the experimental measurement of the variations of electron density behind the shock waves, at the shock velocity range of 7~9km/s, in a low-density shock tube by using the Langmuir electrostatic probe technique. The measurement at such shock velocities is especially useful to validate the calculation model for nonequilibrium processes behind strong shock waves.

## 2 Experimental

The measurement is conducted in a low-density shock tube at the Institute of Mechanics, Chinese Academy of Sciences. The shock tube is made of stainless steel with a driver section 1.6m in length and 22cm in inside diameter. The driven section has a length of 16m and an inside diameter of 80cm. With an aluminium diaphragm of 5mm thick, the shock tube is driven by the combustion of premixed oxygen and hydrogen. Before every run, the driven section is evacuated down to  $1 \times 10^{-5}$  Torr by a turbomolecular pump. The leakage rate is smaller than  $2 \times 10^{-5}$  Torr/min. The time interval from all valves closing to the diaphragm rupture is shorter than 5min. The test gas is prepared by mixing 20% oxygen and 80% nitrogen of purity greater

than 99.998%. The shock tube is run at a fix initial temperature of  $T_1 = 297.2\text{K}$ , but at two different initial pressures of  $P_1 = 0.01$  and  $0.02\text{Torr}$ , respectively. The shock velocities are measured by three ionization detectors mounted in the shock tube wall. Three detectors are positioned 9.5m, 11.5m, and 14m downstream from the diaphragm. A cylindrical Langmuir probe with a radius of 0.05cm and a length of 1cm, made of tungsten and mounted at the axis of the shock tube 14m downstream from the diaphragm, is biased negatively at -9V. The measurement is conducted with the probe axis parallel to the flow velocity to avoid the influence of gas flow on the probe current.

### 3 Langmuir probe

Since the Langmuir probe is biased negatively at -9V, the saturated ion current is collected by the probe. The electron number density can be obtained from the probe data, assuming  $\text{NO}^+$  to be the dominant positive ion within the framework of Laframboise's theory. At the saturated ion current region, the absolute magnitude of the ion current density at the probe surface can be expressed in the form

$$j_i = eN_e \left( \frac{k_B T_e}{2\pi m_i} \right)^{\frac{1}{2}} I_i(x_p, T_i/T_e, r_p/\lambda_D) \alpha(\lambda_D/\lambda_i) \quad (1)$$

where  $j_i$  is the ion current density,  $N_e$  is the electron number density, and  $I_i$  is a dimensionless ion current available in terms of the dimensionless probe potential  $x_p$ , the ratio of the heavy particle temperature to the electron temperature  $T_i/T_e$ , and the ratio of the probe radius to the Debye length  $r_p/\lambda_D$ . In Eq.(1),  $\alpha(\lambda_D/\lambda_i)$  is a correction factor for reduction of the probe current because an ion making collisions within the probe sheath will be subject to an elastic scattering. It is a dimensionless quantity dependent on the average collision number in the probe sheath, which can be expressed as the ratio of the Debye length to the mean ion free path  $\lambda_D/\lambda_i$ .

Sonin[1] recast Laframboise's theory in reducing his data and regarded the dimensionless ion current  $I_i$  as the function of the quantity  $\beta = (r_p/\lambda_D)^2 I_i$  rather than  $r_p/\lambda_D$ . The reason for this is that unlike  $r_p/\lambda_D$  the quantity  $\beta$  is not explicitly dependent on the electron number density and can be calculated directly from the measured  $j_i$  once  $T_e$  has been determined. When  $r_p/\lambda_D \rightarrow \infty$ ,  $I_i \rightarrow 1$ . In fact, when  $\beta > 10^4$ ,  $I_i = 1$  can hold. At the present experiment condition with  $T_e = 2000 \sim 6000\text{K}$  and  $\lambda_D = \left( \frac{k_B T_e}{4\pi e^2 N_e} \right)^{\frac{1}{2}} \approx 10^{-4}\text{cm}$ ,  $\beta > 10^4$  can be arrived at. So we can take  $\alpha = 1$  in interpreting our experimental data.

Schulz & Brown[2] expressed the dependence of the correction factor  $\alpha(\lambda_D/\lambda_i)$  on the average collision number  $\lambda_D/\lambda_i$ . When  $\lambda_D/\lambda_i \ll 1$ ,  $\alpha \rightarrow 1$ . At the present experiment condition, the postshock mean ion free path is estimated as  $\lambda_i \approx 10^{-2}\text{cm}$ , and the average collision number is approximately  $\lambda_D/\lambda_i \approx 10^{-2}$ , so we can take  $\alpha = 1$ .

When the experimental parameters are substituted into Eq. (1), we obtain the postshock electron number density in the form

$$N_e = 9.42 \times 10^{15} I_e^{-\frac{1}{2}} j_i \quad (2)$$

where  $N_e$  is measured in  $\text{cm}^{-3}$  and the probe current density in  $\text{A}/\text{cm}^2$ .

### 4 Electron temperature

It is well known that the air behind a strong shock wave undergoes vibrational excitation, dissociation, and ionization. As a result, the temperatures of the different internal degrees of freedom differ distinctly. According to the probe theory, the controlling temperature for ion collection is

the electron temperature rather than the ion temperature. To determine the electron temperature profile, the postshock states of the air are calculated by using the chemical kinetic scheme including 11 species and Park's three-temperature model[3]. At the experimental condition of  $T_1 = 297.2\text{K}$ ,  $P_1 = 0.02\text{Torr}$ , and shock velocity  $U_S = 7.6\text{km/s}$ , the calculated profile of electron temperature is shown in Fig.1[4].

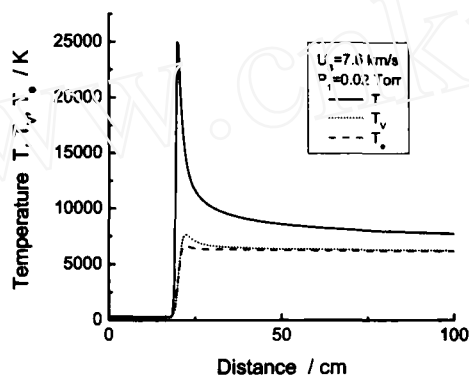


Fig. 1. Calculated temperature profile behind a normal shock wave

## 5 Results

Because there exists a probe current prior to the shock wave arriving, caused by the precursor ionization ahead of strong shock waves, the shock location is determined by extrapolating the region of relatively quick rise in the recorded probe current curve to zero. At the condition of the fix initial pressure  $P_1 = 0.01\text{Torr}$ , and the shock velocities  $U_S = 7.85, 7.85, \text{ and } 7.65\text{km/s}$ , the experimentally obtained electron densities are shown in Fig.2. At the condition of the initial pressure  $P_1 = 0.02\text{Torr}$ , and the shock velocity  $U_S = 8.53\text{km/s}$ , the experimentally obtained electron density is shown in Fig.3. Because the initial pressures are chosen to be relatively low in the present experiment, the relaxation processes to the equilibrium are slow. In Figs.2 and 3, it is seen that the relaxation processes of the electron number density to the equilibrium are interrupted shortly behind the peak by the contact zone arriving. The average peak value of electron density is  $6 \times 10^{12}\text{cm}^{-3}$  in Fig.2, while the peak value is  $1.65 \times 10^{13}\text{cm}^{-3}$  in Fig.3. Both peak values are greater the respective corresponding equilibrium values of electron density of  $3.9 \times 10^{12}\text{cm}^{-3}$  and  $1.2 \times 10^{13}\text{cm}^{-3}$ . The electron density overshoot is verified at the present range of shock velocity. The comparison of the normalized postshock peak values of electron density between the present experiment, Lin's experiment[5] and calculation[6], is shown in Fig.4. It can be seen that the present results are approximately half lower than Lin's theoretical prediction.

In the same manner as in the work of Wilson[7], the characteristic ionization distance is defined by fitting a straight line to the rising portion of the electron density variation, and extrapolating until it intersects with the peak value and zero, as shown in Fig.5. The ionization distances are then divided by the mean free path ahead of the shock wave. For the air, using a **hard-sphere** model, the mean free path ahead of the shock wave becomes  $l_1 = \frac{1.62 \times 10^{14}}{N_t}$ , where  $N_t$  is the total number density in  $\text{cm}^{-3}$ .

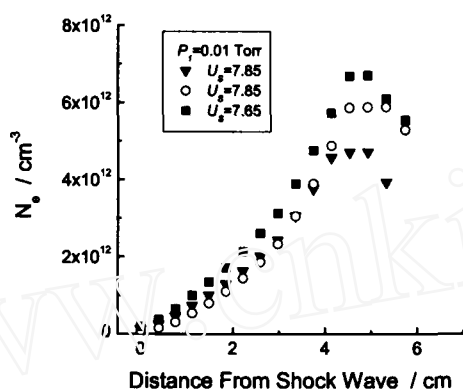


Fig. 2. Electron density profile behind a shock wave for  $P_1 = 0.01$ Torr and  $U_S = 7.65, 7.85$ km/s

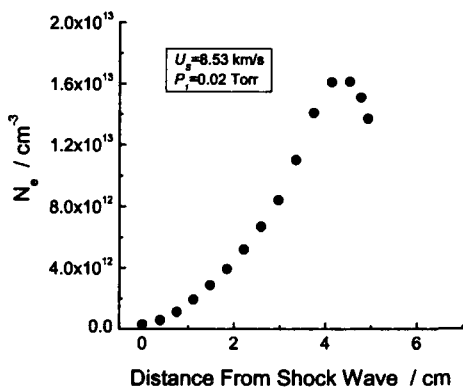


Fig. 3. Electron density profile behind a shock wave for  $P_1 = 0.02$ Torr and  $U_S = 8.53$ km/s

By using his three-temperature model and the some renewed thermochemical parameters, Park[8] calculated the electron density profiles behind shock waves over the velocity range of 2~13km/s. Since the calculated ionization distance is much sensitive to the thermochemical parameters chosen in the calculation, he also made a comparison between the calculated characteristic ionization distances and the existing experimental results[5,7,9,10,11]. In Fig.6, the normalized ionization distances by the mean free path are compared between the present and existing experimental results and Park's calculation. A fairly good agreement is seen here between the two.

## 6 Conclusion

At the shock velocity range of 7~8km/s, which corresponds to the ionization mechanism transition in air, the variations of electron density behind strong normal shock waves are measured in a low-density shock tube using the Langmuir electrostatic probe technique. The electron

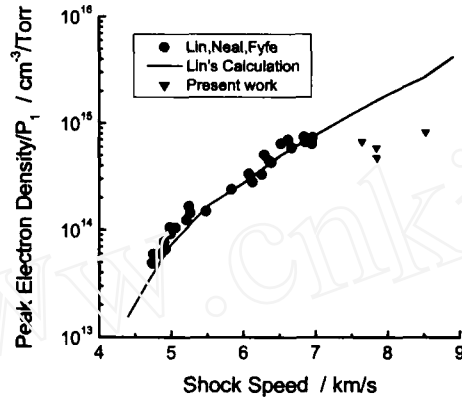


Fig. 4. Comparison between the peak electron densities

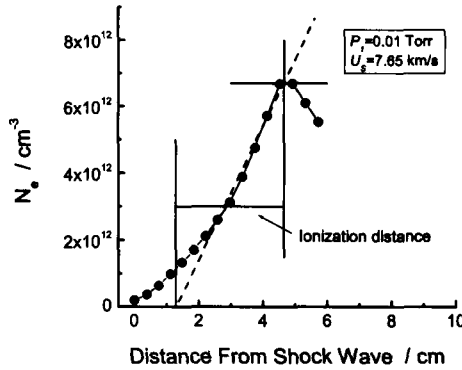


Fig. 5. Characteristic ionization distance for  $P_1 = 0.01\text{Torr}$  and  $U_s = 7.65\text{km/s}$

temperature, calculated based on the Park's three-temperature model, is used to determine the electron density profile behind the strong shock wave. The peak electron densities determined in the present experiment are shown to be half lower than those predicted by Lin's calculation. The experimentally obtained ratios of the characteristic ionization distance to the mean free path of freestream ahead of the shock wave are found to be in a good agreement with the existing experiments and Park's calculation.

## 7 Acknowledgement

Support from the National Natural Science Foundation of China under Grant No.19682008 is acknowledged with thanks.

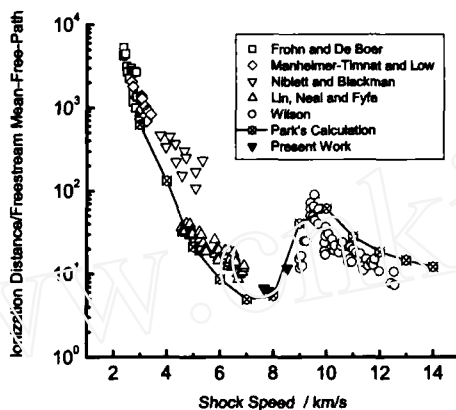


Fig. 6. Comparison between the present work and the existing experiments and Park's calculation

## References

1. A.A. Sonin: Free-molecule langmuir probe and its use in flowfield studies. *J. AIAA* **4**(9), 1588 (1966)
2. G.J. Schulz, S.C. Brown: Microwave study of positive ion collection by probes. *Physical Review* **98**, 1964 (1955)
3. C. Park: On convergence of computation of chemically reacting flows. *AIAA Paper* 85-0247 (1985)
4. H.Y. Zhao, R.L. Zhang, J.L. Le: In: *Proceedings of the 10th Chinese Symposium on Shock Waves, Huangshan, China, Oct. 20-24, 2002*
5. S.C. Lin, R.A. Neal, W.I. Fyfe: Rate of ionization behind shock waves in air. I. experiment results. *Physics of Fluids* **5**(12), 1633 (1962)
6. S.C. Lin, J.D. Teare: Rate of ionization behind shock waves in air. II. Theoretical interpretation. *Physics of Fluids* **6**(3), 355 (1963)
7. J.F. Wilson: Ionization rate of air behind high-speed shock waves. *Physics of Fluids* **9**(10), 1913 (1966)
8. C. Park: Review of chemical-kinetic problems of future NASA missions, I: Earth entries. *J. Thermophysics and Heat Transfer* **7**(3), 385 (1993)
9. A. Frohn, P.C.T. De Boer: Measurement of ionization relaxation times in shock tubes. *Physics of Fluid Supplement I*, I-54-I-57 (1969)
10. Y. Manheimer-Timnat, W. Low: Electron density and ionization rate in thermally ionized gases produced by medium strength shock waves. *J. Fluid Mechanics* **6**, 449 (1959)
11. B. Niblett, V.H. Blackman: An approximate measurement of the ionization time behind shock waves in air. *J. Fluid Mechanics* **4**, 191 (1958)